Electroweak corrections to γZ production at hadron colliders

W. Hollik [a], C. Meier [b]

[a] *Max-Planck-Institut für Physik (Werner-Heisenberg-Institut), D-80805 München, Germany*
[b] *Paul-Scherrer Institut, CH-5232 Villigen PSI, Switzerland*

Abstract

In this Letter we present the results from a calculation of the full electroweak one-loop corrections for γZ vector-boson pair production at hadron colliders. The cases of proton–antiproton as well as proton–proton collisions, at the Tevatron and the LHC, respectively, are considered. Results are presented for the distribution of the γZ invariant mass and for the transverse momentum of the final-state photon. The higher-order electroweak effects are numerically significant, in particular for probing possible anomalous gauge-boson couplings.
© 2004 Elsevier B.V. Open access under CC BY license.

1. Introduction

Experiments at e^+e^- and hadron colliders during the last decade have confirmed the predictions of the Standard Model to very high accuracy (see [1] for a recent review). In particular, the interaction of gauge bosons with fermions has been tested to a precision at the level of 0.1%. On the other hand, one of the most direct consequences of the Standard Model as a non-Abelian gauge theory, the self couplings of the gauge bosons, are known with lower experimental precision. At the LHC, a substantial improvement in the measurement of the vector-boson self couplings will become feasible via the production of gauge-boson pairs providing the best direct tests of the non-Abelian gauge symmetry. Precise predictions from the Stan-

dard Model will allow to isolate possible deviations in the experimental data which may come from anomalous contributions to the gauge self-interactions indicating the presence of new physics beyond the Standard Model. If no deviations are observed, severe bounds on anomalous vector-boson couplings will be obtained (see, e.g., [2] and references therein). Production of neutral vector-boson pairs, like γZ production, is well suited to search for non-zero $ZZ\gamma$ and $Z\gamma\gamma$ couplings, which vanish in the Standard Model, and could thus provide a clean signal of new physics.

Previous studies of γZ pair production in hadronic collisions were first performed at the level of the Born approximation based on the parton processes $q\bar{q} \to \gamma Z$ [3] and were later improved by the NLO QCD corrections [4]. The $O(\alpha_s)$ QCD corrections to the hadronic cross section have been shown to modify the Born result considerably. These corrections are of special importance for high values of the γZ invariant

mass and for high transverse momenta of the photon, i.e., in the regions where also effects from possible anomalous vector-boson self couplings are expected to be identified as deviations from the Standard Model predictions. It is therefore important to have these predictions under control, which makes the inclusion of the higher-order contributions a necessity.

Besides the QCD corrections, electroweak higher-order effects can become significant and have to be taken into account as well. The one-loop logarithmic electroweak effects in WZ and $W\gamma$ production have been studied in [5]. Here we consider the hadronic production of γZ pairs and present a calculation of the full electroweak one-loop corrections to the parton processes $q\bar{q} \rightarrow \gamma Z$ and to the hadronic cross section and distributions. Applying appropriate kinematical cuts, numerical results are given for the invariant-mass distribution of γZ and for the photon transverse momentum, in PP collisions at the LHC as well as in $P\bar{P}$ collisions at the Tevatron.

2. Parton processes

At the partonic level, pair-production of neutral vector bosons in lowest order can only proceed via quark–antiquark annihilation, $q\bar{q} \rightarrow \gamma Z$ ($q = u, d, s, c, b$). NLO electroweak corrections consist of the one-loop virtual contributions and the contributions from real-photon bremsstrahlung. The subclass of loop diagrams involving virtual photons gives rise to infrared (IR) divergences; these are cancelled by including real-photon emission off the quark lines and integrating over the photon phase space. In the NLO-order electroweak contribution to the partonic cross section, $d\sigma_{q\bar{q}}^{(1)}$, it is convenient to separate the QED corrections from the residual part of the purely weak corrections,

$$d\sigma_{q\bar{q}}^{(1)} = d\sigma_{q\bar{q}}^{\mathrm{weak}} + d\sigma_{q\bar{q}}^{\mathrm{QED}}, \tag{1}$$

with the QED part split according to

$$d\sigma_{q\bar{q}}^{\mathrm{QED}} = d\sigma_{q\bar{q},\mathrm{virt}}^{\mathrm{QED}} + d\sigma_{q\bar{q},\mathrm{real}}^{\mathrm{QED}}. \tag{2}$$

Such a separation like in (1) appears natural for neutral–current processes since the virtual QED corrections form a gauge-invariant subset of the full one-loop diagrams; they are defined as the sum of the di-

agrams displayed in Fig. 1. Moreover, they are UV-finite when quark wave-function renormalization and mass renormalization, both exclusively from virtual photons, are taken into account, as indicated in the third line of Fig. 1.

The QED corrections still contain mass-singular large logarithms of the type $\log \hat{s}/m_q^2$ (with the invariant mass squared $\hat{s}$ of the parton process) arising from real and virtual photons collinear to a quark or anti-quark with mass m_q. These singular terms are universal and can be absorbed by a redefinition of the parton distributions functions (PDFs) of the initial-state quarks. By this procedure, the mass singularities disappear from the observable cross section, and the renormalized PDFs become dependent on the factorization scale μ_F, controlled by the Gribov–Lipatov–Altarelli–Parisi (GLAP) equations [6]. Those universal photonic corrections can be taken into account by a modification of the GLAP equations of QCD introducing an additional QED-evolution term [7]. This leads to small corrections to the PDFs, at the per mill level [2].

The consistent treatment of the QED corrections would also require the inclusion of QED corrections in all the data used for global fitting of the PDFs. Current determinations of PDFs [8,9] do not include QED corrections, inducing thus an uncertainty which, however, should be small compared to the present uncertainties on the PDFs.

Absorbing the collinear singularities associated with initial-state photon radiation into the PDFs introduces a QED factorization-scheme dependence. Our calculation is based on an explicit diagrammatic evaluation, with the collinear singularities factorized according to the $\overline{\mathrm{MS}}$ scheme [10], but QED corrections are not taken into account in the PDF evolution.

For the residual class of purely weak corrections, one only encounters loop diagrams and counter terms with massive virtual particles. Note that also in the counter terms for quark mass and wave-function renormalization all virtual photon contributions have been separated off as part of the QED corrections. The counter terms are determined by the electroweak renormalization scheme, which we choose as the on-shell scheme [11,12]. The partonic cross section derived from the renormalized set of weak loop diagrams is hence UV-finite and does not contain any collinear or infrared divergences. The practical
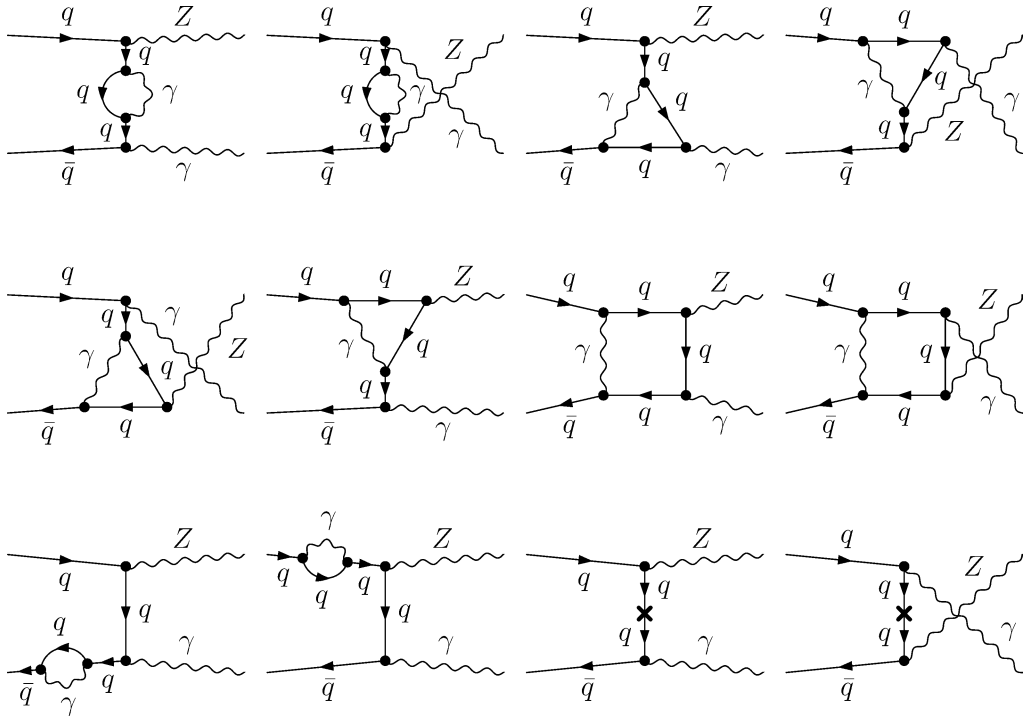
Fig. 1. One-loop diagrams with virtual photons (virtual QED contributions). The cross marks the QED mass-renormalization counter term from the virtual photon contribution to the quark self-energy.

computation and evaluation of the complete one-loop terms was done with support of the packages FeynArts and FormCalc [13], where the version [12] of the on-shell renormalization scheme is implemented.

3. Hadronic observables

The observable hadronic cross section for $P + P(\bar{P}) \to \gamma + Z + X$, with a given total hadronic CMS energy $\sqrt{S}$, can be written as a convolution of the parton cross sections with the corresponding parton luminosities and summation over the various parton species. The one-loop order partonic cross section for $q\bar{q}$ annihilation is obtained from the lowest-order cross section $d\sigma_{q\bar{q}}^{(0)}$ and the NLO contribution (1) after factorization of the collinear photon contributions in the QED part at the scale μ_F,

$$
d\sigma_{q\bar{q}}^{(0+1)}(\hat{s}, \hat{t}) = d\sigma_{q\bar{q}}^{(0)}(\hat{s}, \hat{t}) + d\sigma_{q\bar{q}}^{\text{weak}}(\hat{s}, \hat{t})
$$
$$
+ d\sigma_{q\bar{q}}^{\text{QED}}(\hat{s}, \hat{t}, \mu_F), \tag{3}
$$

with the invariant kinematical variables $\hat{s}$ for the partonic CMS energy squared and $\hat{t}$ for the momentum transfer between q and γ. Integration over $\hat{t}$ (applying appropriate cuts as described below) yields the hadronic cross section in the following way,

$$
\sigma_{AB}^{\gamma Z}(S) = \int_{\tau_0}^{1} d\tau \sum_{u\bar{u}, d\bar{d}, \dots} \frac{d\mathcal{L}_{q\bar{q}}^{AB}}{d\tau} \sigma_{q\bar{q}}^{(0+1)}(\tau S), \tag{4}
$$

with the parton luminosity

$$
\frac{d\mathcal{L}_{q\bar{q}}^{AB}}{d\tau} = \int_{\tau}^{1} \frac{dx}{x} \left[q_A(x, \mu_F) \bar{q}_B \left(\frac{\tau}{x}, \mu_F \right) \right.
$$
$$
\left. + \bar{q}_A(x, \mu_F) q_B \left(\frac{\tau}{x}, \mu_F \right) \right], \tag{5}
$$

where $q_A(x, \mu_F)$ $[\bar{q}_A(x, \mu_F)]$ denote the density functions for the quarks [antiquarks] in the hadron A carrying a fraction x of the hadron momentum at the scale μ_F; $(A, B) = (P, P)$ for the LHC and $(P, \bar{P})$ for the Tevatron. The lower bound of the τ-integration (τ_0)

Table 1
Input parameters for the kinematical variables and the Higgs boson mass entering the numerical evaluation

	$\sqrt{S}$ (TeV)	$p_{\mathrm{T}}^{\gamma,c}$ (GeV)	$y^{\gamma,c}$	M_H (GeV)
LHC	14	100	2.4	115
Tevatron	1.8	10	2.4	115

determines the minimal invariant mass of the parton system, $\hat{s}_0 = \tau_0 S$. In our case, τ_0 depends on the kinematical cuts applied. In order to have sufficiently large transverse photon momenta not too close to the beam axis, the following cuts

$$p_{\mathrm{T}}^{\gamma} > p_{\mathrm{T}}^{\gamma,c}, \qquad \left| y^{\gamma} \right| < y^{\gamma,c}, \tag{6}$$

are imposed for the photon transverse momentum p_{T}^{γ} and for the pseudo-rapidity y^{γ} of the photon, defined by

$$y^{\gamma} = -\log\left(\tan\frac{\theta}{2} \right), \tag{7}$$

where θ is the scattering angle in the laboratory frame. The p_{T}^{γ} cut implies an energy and angular cut in the parton CMS,

$$\hat{s} > \tau_0 S = \left(p_{\mathrm{T}}^{\gamma,c} + \sqrt{(p_{\mathrm{T}}^{\gamma,c})^2 + M_Z^2} \right)^2,$$

$$|\cos\hat{\theta}| < \sqrt{1 - \frac{4\hat{s}(p_{\mathrm{T}}^{\gamma,c})^2}{(\hat{s} - M_Z^2)^2}}. \tag{8}$$

In the laboratory frame, $|y^{\gamma}|$ can still become quite large. Then, the additional y^{γ} cut restricts photons from coming too close to the beam axis in the laboratory frame. Assignment of specific values for the minimum p_{T}^{γ} and maximum $|y^c|$, as used in our numerical analysis, are contained in Table 1.

Observables of particular interest are the distribution for the invariant mass $M_{\mathrm{inv}}^{\gamma Z} = \sqrt{\hat{s}}$ of the γ–Z final state configuration,

$$\frac{d\sigma_{AB}^{\gamma Z}}{dM_{\mathrm{inv}}^{\gamma Z}} = \frac{2M_{\mathrm{inv}}^{\gamma Z}}{S} \sum_{q,\bar{q}} \frac{d\mathcal{L}_{q\bar{q}}^{AB}}{d\tau} \sigma_{q\bar{q}}^{(0+1)}(\tau S), \tag{9}$$

and the distribution for the photon transverse momenta,

$$\frac{d\sigma_{AB}^{\gamma Z}}{dp_{\mathrm{T}}^{\gamma}} = \int_{\tau_0}^{1} d\tau \sum_{q,\bar{q}} \frac{d\mathcal{L}_{q\bar{q}}^{AB}}{d\tau} \frac{d\sigma_{q\bar{q}}^{(0+1)}}{dp_{\mathrm{T}}^{\gamma}}(\tau S, p_{\mathrm{T}}^{\gamma}). \tag{10}$$

The kinematical constraints arising from the cuts divide the phase space into several subvolumes, over each of which is integrated separately. Integration over phase space was done numerically. To test the stability of the numerical integration, the results from an adaptive Gauss algorithm were checked versus those obtained from the Monte Carlo routine VEGAS7. As a further check, our results for the hadronic cross section in Born approximation were compared with the results of the earlier calculations in [3].

4. Numerical evaluation

The results of the numerical analysis are of lowest order with respect to QCD in the parton processes. Hence, the numerical values are not yet the real predictions from the Standard Model; they are given here to point out and illustrate the effects of the higher-order electroweak contributions. The input parameters and the kinematical cuts have been chosen as listed in Table 1, together with the factorization scale $\mu_F = 2M_Z$.

QED and weak corrections were calculated separately. As already mentioned above for the QED corrections, the collinear singularities were factorized according to the $\overline{\mathrm{MS}}$ scheme, but QED corrections are not taken into account in the quark distribution functions used for our analysis [8]. The residual non-singular QED corrections are quite small, at the level of 0.5%. There is, however, a left-over QED factorization-scale dependence, as a consequence of the missing QED evolution of the PDFs. This induces a scale uncertainty which is of the order of a few per mill as well. The calculation of the QED contributions thus provides more an estimate of the order of magnitude rather than precise numbers. From a practical point of view, the QED effects for γZ production are negligible since they are small and covered up by the uncertainties of the quark distribution functions.

The class of weak corrections induces more significant effects, in particular in those regions that are of interest for testing possible anomalous gauge couplings [2]. Sensitive observables for the analysis of anomalous vector-boson couplings are the distributions of the hadronic cross sections in terms of the invariant mass of γ and Z as well as the distribution of the transverse momentum of the final state photon.
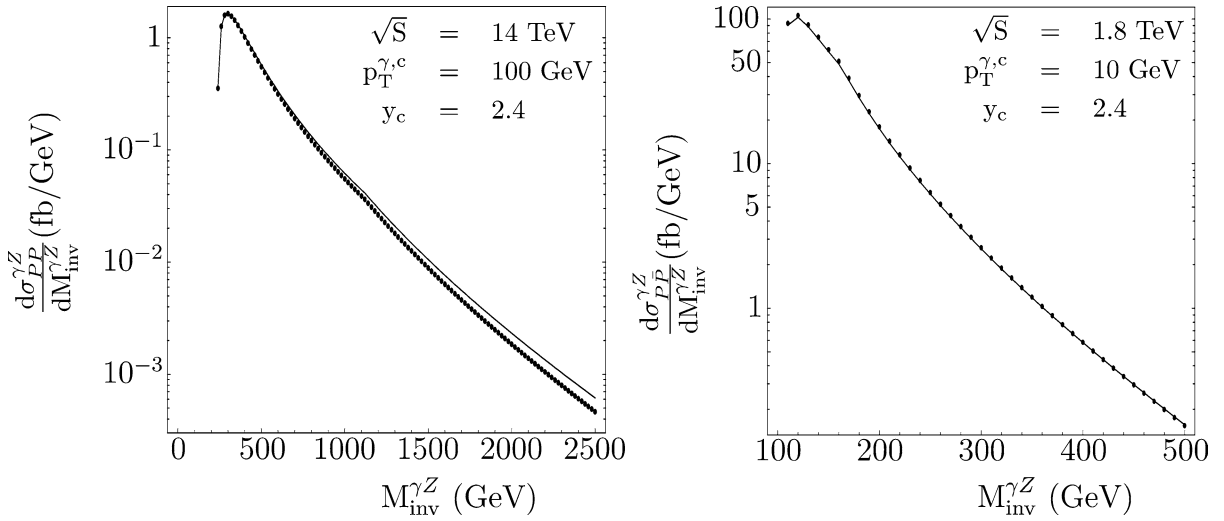
Fig. 2. Distribution of the γZ invariant mass in Born approximation (solid line) and including the full one-loop electroweak corrections (dotted line), for the LHC (left case) and for the Tevatron (right case).
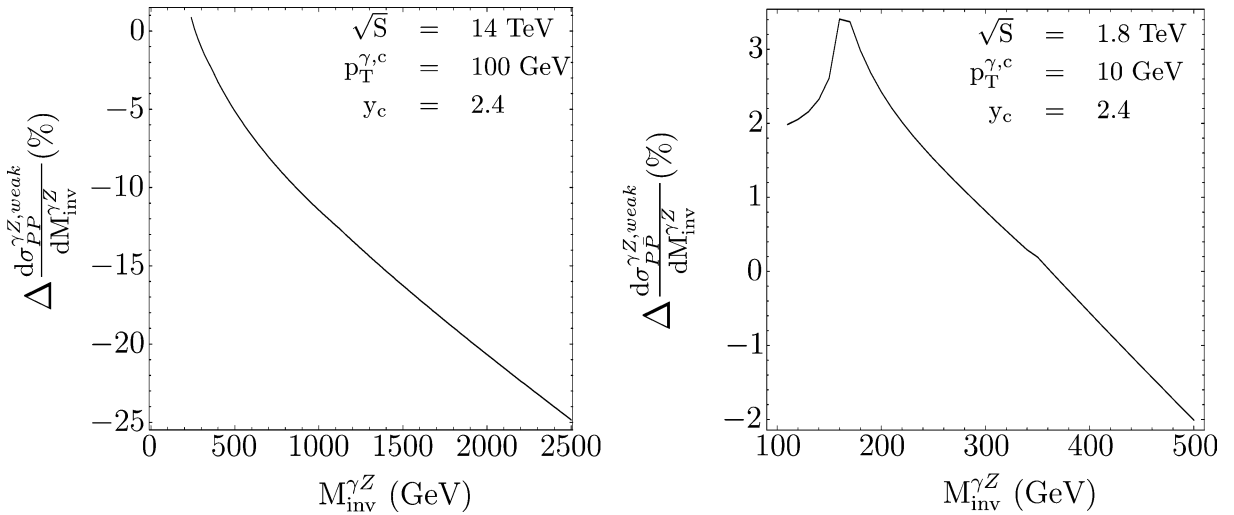
Fig. 3. Weak corrections to the distribution of the γZ invariant mass relative to the Born result, for the LHC (left case) and for the Tevatron (right case).

To illustrate the electroweak higher-order effects, we show in Fig. 2 the distribution of the γZ invariant mass in lowest-order approximation in comparison to the corresponding result including the full one-loop electroweak corrections, both for the LHC and for the Tevatron. To be more quantitative, Fig. 3 displays the purely weak corrections to the $M_{\text{inv}}^{\gamma Z}$ distribution, relative to the Born result. In the LHC case, the weak corrections reach a considerable size around 20% for

high invariant masses, whereas for the Tevatron they are in the lower percentage region.

In a similar way, in Figs. 4 and 5, the corresponding results are shown for the p_T distribution of the final-state photon. Again, the weak contributions are sizeable in case of the LHC, at the level of 30% and more for high p_T^{γ}. But also for the Tevatron case, they can exceed the level of 10%. The origin of the large effects at high invariant masses or high p_T,
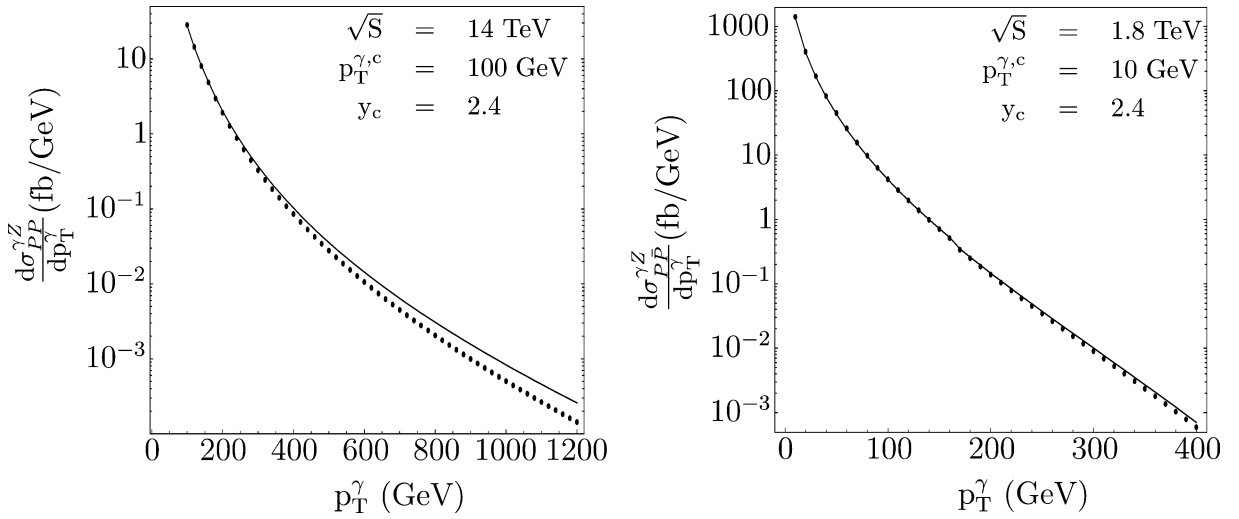
Fig. 4. Distribution of the transverse momentum in Born approximation (solid line) and including the full one-loop electroweak corrections (dotted line) for the LHC (left case) and for the Tevatron (right case).
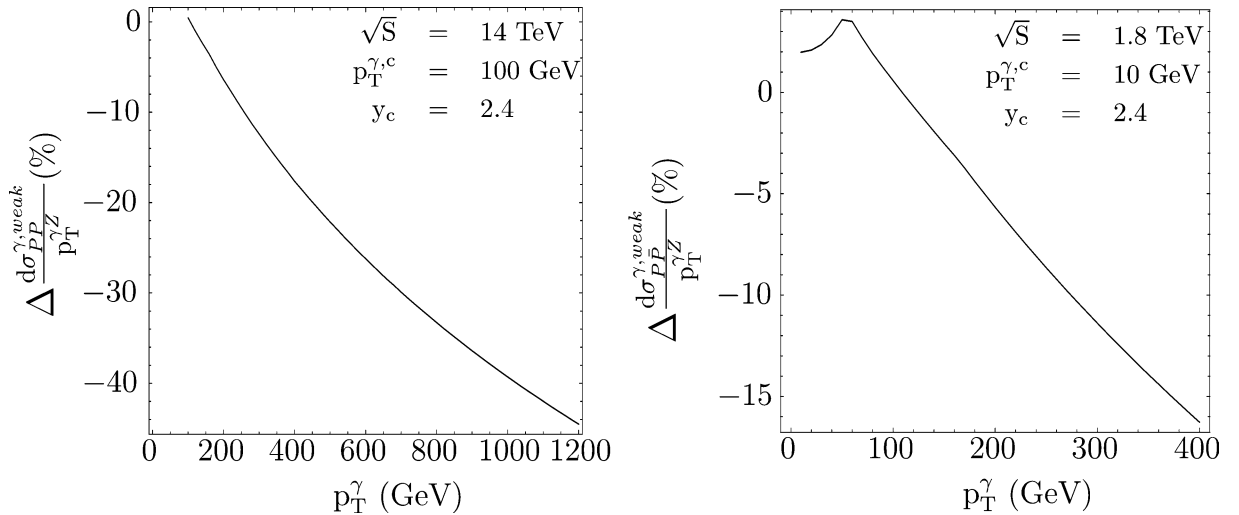

Fig. 5. Weak corrections to the distribution of the transverse momentum relative to the Born result, for the LHC (left diagram) and for the Tevatron (right diagram).

respectively, are large logarithms, e.g., of the type $\alpha \log^2(\hat{s}/M_Z^2)$, in the one-loop contributions to the parton processes.

Finally, the electroweak loop terms depend also on the mass of the Higgs boson, which was kept at $M_H = 115$ GeV for the numerical results displayed in the figures. The dependence on M_H is not very strong, yielding a variation of a few per cent (relative) of the electroweak corrections setting $M_H = 1$ TeV.

The electroweak corrections are negative whenever they are sizeable, opposite to the positive NLO QCD corrections [4], and thus partially compensate the NLO QCD contributions.

To summarize, we have presented the results of a full electroweak one-loop calculation for the production of γZ pairs at hadron colliders, evaluated for both the Tevatron and the LHC. Like for other neutral–current processes, the electroweak $O(\alpha)$ corrections

naturally decompose into QED and weak contributions, which are separately gauge invariant and UV-finite. The QED corrections, arising from virtual and real photon emission, contain collinear singularities which are factorized and absorbed in the PDFs. The remaining QED corrections are small, below the percent level, and insignificant in view of the uncertainties of the quark distribution functions. The weak corrections, however, are sizeable for large parton energies or transverse photon momenta, respectively, especially for the LHC, and have to be taken into account together with the NLO QCD corrections for testing the gauge structure of the Standard Model and probing the existence of anomalous gauge couplings.

Acknowledgements

References

[1] LEP Collaborations: ALEPH, DELPHI, L3, OPAL, LEP Electroweak Working Group, SLD Electroweak and Heavy Flavour Working Groups, hep-ex/0312023;
M. Grünewald, Electroweak physics, in: Proceedings of the 31st International Conference on High Energy Physics, Amsterdam, 2002, hep-ex/0210003.

[2] S. Haywood, P.R. Hobson, W. Hollik, Z. Kunszt, et al., Electroweak physics, in: G. Altarelli, M.L. Mangano (Eds.), Proceedings of the 1999 CERN Workshop on SM Physics (and More) at the LHC, CERN 2000-004, hep-ph/0003275.

[3] J.J. van der Bij, E.W.N. Glover, Phys. Lett. B 206 (1988) 701;
U. Baur, E.W.N. Glover, Nucl. Phys. B 318 (1989) 106.

[4] U. Baur, T. Han, J. Ohnemus, Phys. Rev. D 57 (1998) 2823;
J.M. Campbell, R.K. Ellis, Phys. Rev. D 60 (1999) 113006;
L. Dixon, Z. Kunszt, A. Signer, Phys. Rev. D 60 (1999) 114037;
D. De Florian, A. Signer, Eur. Phys. J. C 16 (2000) 105.

[5] E. Accomando, A. Denner, S. Pozzorini, Phys. Rev. D 65 (2002) 073003.

[6] V.N. Gribov, L.N. Lipatov, Sov. J. Nucl. Phys. 15 (1972) 438;
V.N. Gribov, L.N. Lipatov, Sov. J. Nucl. Phys. 15 (1972) 675;
G. Altarelli, G. Parisi, Nucl. Phys. B 126 (1977) 298.

[7] H. Spiesberger, Phys. Rev. D 52 (1995) 4936.

[8] A. Martin, R.G. Roberts, J. Stirling, Phys. Lett. B 354 (1995) 155;
A. Martin, R.G. Roberts, J. Stirling, R. Thorne, Eur. Phys. J. C 4 (1998) 463.

[9] H. Lai, et al., CTEQ Collaboration, Eur. Phys. J. C 12 (2000) 375.

[10] U. Baur, S. Keller, D. Wackeroth, Phys. Rev. D 59 (1999) 013002.

[11] M. Böhm, W. Hollik, H. Spiesberger, Fortschr. Phys. 34 (1986) 687;
W. Hollik, Fortschr. Phys. 38 (1990) 165.

[12] A. Denner, Fortschr. Phys. 41 (1993) 307.

[13] J. Küblbeck, M. Böhm, A. Denner, Comput. Phys. Commun. 60 (1990) 165;
T. Hahn, Comput. Phys. Commun. 140 (2001) 418;
T. Hahn, M. Perez Victoria, Comput. Phys. Commun. 118 (1999) 153.